Proceedings of PSFVIP-2
May 16-19, 1999, Honolulu, USA
PF109

Thickness and Slope Measurements of Thin Liquid Film To an Accuracy of λ/4 Using Fizeau Interferometry

Kenneth D. Kihm
Department of Mechanical Engineering
Texas A&M University, College Station, Texas 77843-3123, USA
E-mail: ken-kihm@tamu.edu
David M. Pratt
Wright-Patterson Air Force Laboratory
Dayton, Ohio 45433-7542, USA

This paper presents a new optical technique to measure thin liquid film thickness and slope based on the principle of Fizeau interferometry. The interferometric fringes, constructed by the two reflected rays respectively from the solid-liquid and liquid-vapor interfaces, allow measurement of the thin film thickness at an accuracy of λ/4 when a monochromatic light source (λ = 520 nm) is used. When a white light source is used, colored interferometric fringes are formed and their color spectrum is constructed in different orders depending on the slope of film thickness, i.e., the spectrum order in R-Y-G-B indicates a negative slope of the film thickness and the order in R-B-G-Y indicates a positive slope of the thickness. Also, a micro-scale extension and movement control of the thin film region, using an electrohydrodynamic (EHD) phoresis, is first demonstrated and visualized.

INTRODUCTION

Some commercial and military applications in terrestrial and space thermal management systems require heat transport and dissipation capabilities in the hundreds of watts per square centimeter level. Of the heat transport devices presently under consideration in this regime, most utilize liquid-vapor phase change due to its superior heat transfer characteristics which can translate to a system with a reduced mass and at a near constant temperature. Additionally, if the phase change device is capillary-driven, the device will be passive, requiring no mechanical circulator for the working fluid.

The broad category of capillary-driven heat transfer devices includes capillary pumped loops (CPL). Figure 1 shows a simple CPL that is composed of a single pore evaporator and a single pore condenser. In this figure, Q_e and Q_c are the heat transferred into and out of the CPL, respectively. Heat addition to the evaporator section of CPL results in evaporation from the thin film region of the meniscus. The vapor flows to the condenser section where the removal of heat causes the vapor to condense. The liquid is driven back to the evaporator through the capillary pressure differential between the pores of different diameters. When evaporation exceeds the rate of liquid re-supply, the device is said to reach its capillary limit and fails. Thus, the capillary limit has been typically used to define the maximum heat transfer capability of CPL. In practice, the maximum heat transfer capability associated with

the capillary limit is rarely achieved [1]. The basic mechanisms describing evaporating menisci in CPL at the capillary limit are not fully understood to date.

Although the capillary pore dimensions are generally in macroscopic order of one millimeter, the most of energy and mass transport of CPL is known to occur within the microscale region of the liquid meniscus near the three phase contact point [2]. The liquid meniscus extends to the molecular level of an order of sub-nanometer thickness along a clean solid surface (Fig. 2). In this adsorbed film layer, the strong Van-der-Waals attractions prohibit any evaporative flux of liquid molecules. When the layer thickness exceeds a certain limit, called a bulk meniscus region, the evaporative flux is again negligible since the meniscus surface temperature is not high enough for active evaporation. In between, called a thin film region, most evaporation occurs and its peak has been predicted to be closely located to the boundary of the adsorbed film region [3,4].

The essential characteristics of the evaporating meniscus are sub-micron scale phenomena and the most energy and mass transport occurs within the thin film region of a few micron length with a submicron thickness [2-4]. Because of the experimental difficulties associated with the extremely small scale of the region of our interest, majority of the previous studies has been done analytically and numerically. Dynamics associated with the micro-scale fluid motion and concentrated heat transport in the vicinity of the evaporating meniscus front can crucially affect the driving capillary potential by altering the wetting ability of the working fluid [5]. The change in wettability results in changes of the thin film thickness and slope, and in turn, the micro-scale dynamics are significantly governed by the micro-scale characteristics of the thin film region where most energy and mass transport occurs in CPL.

Therefore, a precise determination of the thickness variations of thin liquid film near the meniscus front is necessary to consider augmentation of the heat transfer efficiency of CPL. Also, the microscale extension and movement control of the thin film region, if ever nonintrusively possible, will be very beneficial to enhance the energy and mass transfer of CPL. An electrohydrodynamic (EHD) phoresis shows a potential of the micro-scale control of the thin film behavior. A successful implementation of the nonintrusive control of the thin film region movement can counter-balance the meniscus instability and prevent the evaporator dryout from occurring at high energy and mass transport conditions of CPL.

EXPERIMENTAL METHODOLOGY

Figure 3 illustrates the Fizeau interferometry [6] for micro-scale measurements that basically consists of a microscopic imaging system with a monochromatic light source. The top surface of the test cell is made of a thin and flat glass plate. The monochromatic light ray partially reflects from the inner surface of the top glass plate and partially reflects from the liquid-vapor interface, as shown in the inset drawing. These two reflected rays create an optical path length differential, 2δ, equivalent to two times the meniscus thickness. When the optical path length differential, 2δ is equivalent to $m\lambda$ (m = 1, 2, 3,...), the two rays interfere constructively and the resulting light intensity is the highest. When the optical path length differential 2δ is equivalent to $(m+1/2)\lambda$, the two rays interfere destructively and the darkest intensity is resulted. The resulting sinusoidal intensity patterns construct optical fringes. Thus, the successive brightest and darkest locations on the fringes represent thickness differentials of one-quarter of the wavelength, $\lambda/4$ = 95.8 nm. Note that λ represents the liquid medium wave length, i.e., $\lambda = \lambda_o/n$ where the incident light wave length in vacuum, λ_o = 520 nm, and the refractive index of the tested liquid pentane (C_5H_{12}) is taken for n = 1.357 at 20°C.

Additional noble feature of the experiment innovates an idea of using unfiltered white light source to determine the thickness gradient of thin film. The visible light spectrum ranges from 400 nm to near 700 nm consisting colors ranging from purple, blue, green, yellow, orange to red. Also, the Fizeau fringes are broadened by the color spectrum and the order of the spectrum depends on the film thickness gradient, i.e., red-shifted for relatively thicker film regions and blue-shifted for relatively thinner film regions (Fig. 4). Therefore, when the film thickness decreases along a certain direction, the order of color fringes along the same direction will be red, yellow, green, blue, red, yellow, green, blue, red, ... repeating the cycles. On the other hand, when the film thickness increases, the order will be reversed, i.e., red, blue, green, yellow, red, and so on. Therefore, by carefully analyzing the fringe color orders, the film thickness contour mapping can be completed including the thickness slope.

The rectangular test cell (Fig. 5-a) is made of two 105 mm square, 1 mm thick flat glass plates spaced 8 mm apart. Figure 5-b shows the electrode configuration, attached to the top glass surface of the test cell, to examine the feasibility of electrohydrodynamic (EHD) phoresis moving and extending the thin film region of the meniscus. The net force that arises due to the action of the electric field can be shown to be [7]

$$F_e = qE + Const_1 \nabla E^2 + Const_2 E^2 \nabla \kappa \qquad (1)$$

where q is the electric field space charge density, E is the applied electric field strength, κ is the dielectric constant, and $Const_1$ and $Const_2$ are given by the electric properties of tested fluid. The first term on the right side of Eq. (1) presents Coulomb force for ionized molecules. In highly dielectric fluids with low dielectric permittivity, such as pentane, the EHD current discharge is negligible and therefore the first term is insignificant. The second and third terms present forces resulting because of nonuniformity of the electric field and nonuniformity in the dielectric permittivity of the fluid, respectively. If there is no spatial variation in the dielectric constant, where $\nabla \kappa = 0$ and the third term is negligible, the EHD force will be solely determined by the nonuniformity in the electric field. Since the net electric force F_e is proportional to the gradient of the scalar amount of E^2, the fluid molecules will always move toward the electrode of the higher electric field, regardless of its polarity. This phenomenon is called *dielectrophoresis*. The saw teeth shape electrode is located above the meniscus so that the thin film is always attracted by its highly stressed and nonuniform electric field (Fig. 5-b).

RESULTS AND DISCUSSION

Typical Fizeau fringes for the thin film region of Pentane (σ = 15.5 dyne/cm, κ = 1.84, ρ = 621.4 kg/m^3, M (molar mass) = 72.15 kg/mole, T_{boiling} = 309 K or 36°C), under no surface heating, are shown for monochromatic light illumination (λ = 520 nm) in Fig. 6-a, and for white light illumination (400nm < λ < 700 nm) in Fig. 6-b. The bulk meniscus region is located to the left of the image field. The entire fringes in the right region of the center wider one will disappear once the surface is heated by a foil heater and the thin film evaporation is established. Therefore, we believe that these fringes represent the condensed liquid layer under a subcooled environment provided by the cooler glass surface. The center wider fringe will turn into the evaporating meniscus front of the three phase contact point after the surface heater evaporates off the condensed surface layer in the right hand side region.

Figure 6-a was digitized and scanned for the pixel gray levels along a specified direction, for example, in perpendicular to the fringe orientation. The peaks and valleys of the resulting sinusoidal intensity profiles correspond to the locations of $\lambda/4$ thickness differential. Figure 6-b provides an information on the thickness slope variation. For example, the fringe colors, from left to right with respect to the green on at the center, change in order of R-Y-G-Y-R. Indexing to the color code shown in Fig. 4, we can determine that the center green fringe corresponds to the thinnest valley location and the film thickness increases in both directions away from the center. Figure 7 shows the quantitative result of the fringe analysis for the film thickness versus the *x*-location measured from left to right. Note that the apparent film thickness in the coordinate is multiplied by the liquid index of refraction, presently $n = 1.357$ for pentane, and the actual film thickness must be thinner by the factor of n than the apparent thickness.

Figure 8 compares three different CCD images taken for menisci formed under different heating and electric charging conditions. The full-view fringes shown in Fig. 8-a, under zero heating, $Q = 0$, and zero charging voltage, $V_{ch} = 0$, are divided by the center wider fringe, the left of which shows the thin film region and the right of which shows the subcooled condensed layer. When the condensed film is dried off by the surface heating at $Q = 0.2$ W (Fig. 8-b), the right side fringes disappear and only the left side fringes, representing the thin evaporating film region, remain. The location of the wider center fringe in Fig. 8-a now recedes to the evaporating meniscus front in Fig. 8-b. In addition to the surface heating, when the pentane is charged by the surface electrodes at $V_{ch} = 1.5$ kV, the EHD phoresis moves the meniscus front to the right toward the serrated electrode that creates highly nonuniform electric field gradient.

The beginning of the first dark fringe, either in Fig. 8-b or c, is taken as the evaporating meniscus front of zero thickness. The center of the first dark fringe indicates the location of the film thickness, $\delta = \lambda/4$ or 95.8 nm, and the center of the first bright fringe indicates $\delta = \lambda/2$ or 191.6 nm. The centers of the second dark and bright bands are equivalent to $\delta = 287.4$ nm and 383.2 nm, respectively, and so on. Since the neighboring (dark or bright) fringes get narrower as we go to the left, the meniscus slope shows a gradual increase toward the bulk meniscus region. The results of the fringe analysis for the film thickness profiles are shown for different charging voltages under no heating in Fig. 9-a and under a constant surface heating of 0.2 W in Fig. 9-b. The amount of electrophoresis increases with increasing charging voltage regardless of the surface heating.

CONCLUSION

Capillary pumping loop (CPL) heat exchanger device is known to have its most energy and mass transport occur through the thin film region of an order of 1 μm length and sub-micron thickness within its evaporating meniscus front. Noble diagnostic methods have been developed and used to determine the complete contours of thin film thickness variations of both evaporating and nonevaporating pentane menisci. Also, the developed visualization technique has evidenced the electrophoresis of the thin film and first demonstrated the potential for the nonintrusive and micro-scale control of the thin film, which can contribute to devise quenching the meniscus instability growth occurring at high heating rates.

Primary conclusions reached from the present study are:

1. Monochromatic light Fizeau interferometry system has been successfully developed to measure the thickness of thin liquid film to the resolution of $\lambda/4$.
2. White light Fizeau interferometry system has been first devised to determine the thin film thickness gradient to complete the contour mapping of the film thickness variation.

3. Active control of the meniscus front and extension of the thin film region have been first achieved and visualized by the use of electrohydrodynamic (EHD) phoresis with specially designed electrodes.

REFERENCES

1. R. Richter and J. M. Gottschlich, Thermodynamic Aspects of Heat Pipe Operation, *Journal of Thermophysics and Heat Transfer*, vol. 8, no. 2, pp. 334-340, 1994.
2. M. Potash and P. C. Wayner, Evaporation from a Two-Dimensional Extended Meniscus, *Int. J. Heat Mass Transfer*, vol. 15, pp. 1851-1863, 1972.
3. A. Mirzamoghadam and I. Catton, A Physical Model of the Evaporating Meniscus, J. Heat Transfer, vol. 110, pp. 201-207, 1988.
4. F. J. Renk and P. C. Wayner, An Evaporating Ethanol Meniscus, Part II: Analytical Studies, *J. Heat Transfer*, vol. 101, pp. 59-62, 1979.
5. D. M. Pratt and K. P. Hallinan, Thermocapillary Effects on the Wetting Characteristics of a Heated Curved Meniscus, *Journal of Thermophysics and Heat Transfer*, vol. 11, no. 4, pp. 519-525, 1997.
6. E. Hecht, *Optics*, Addison-Wesley, New York, 1987.
7. A. Singh, , Eletrohydrodynamic (EHD) Enhancement of In-Tube Boiling and Condensation of Alternate (Non-CFC) Refrigerants, Ph.D. Dissertation, University of Maryland, College Park, MD, 1995.

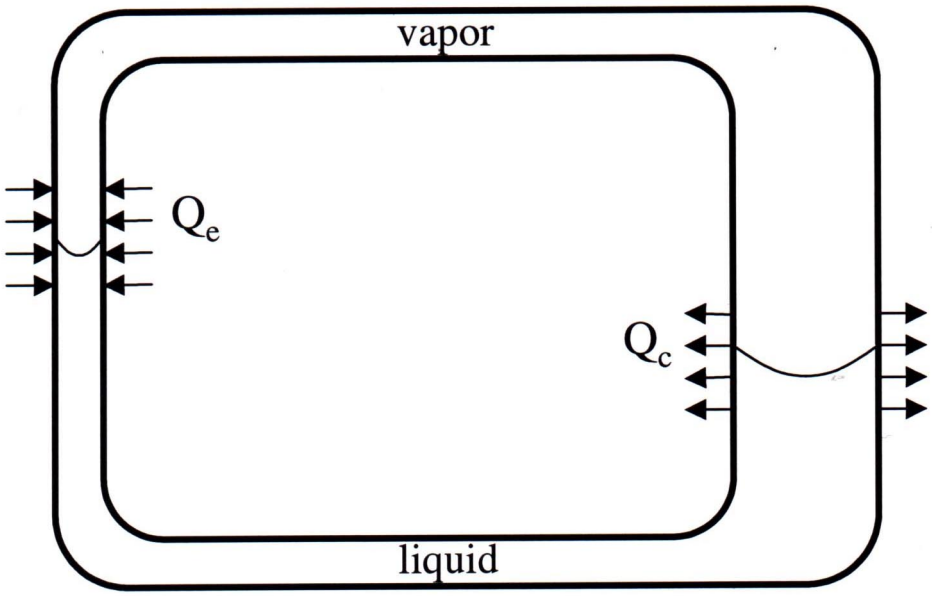

Fig. 1 Capillary pumping loop (CPL).

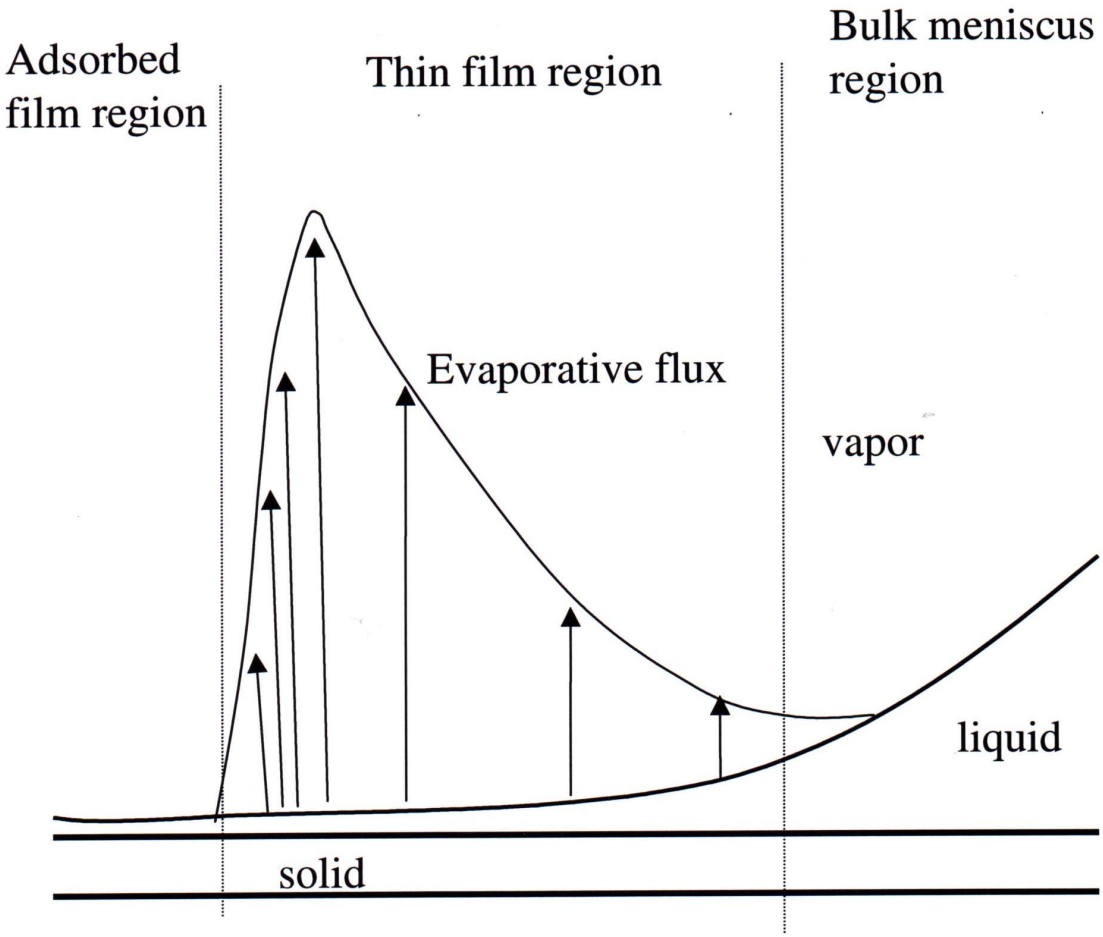

Fig. 2 Development of meniscus and evaporative flux distribution along a heated surface

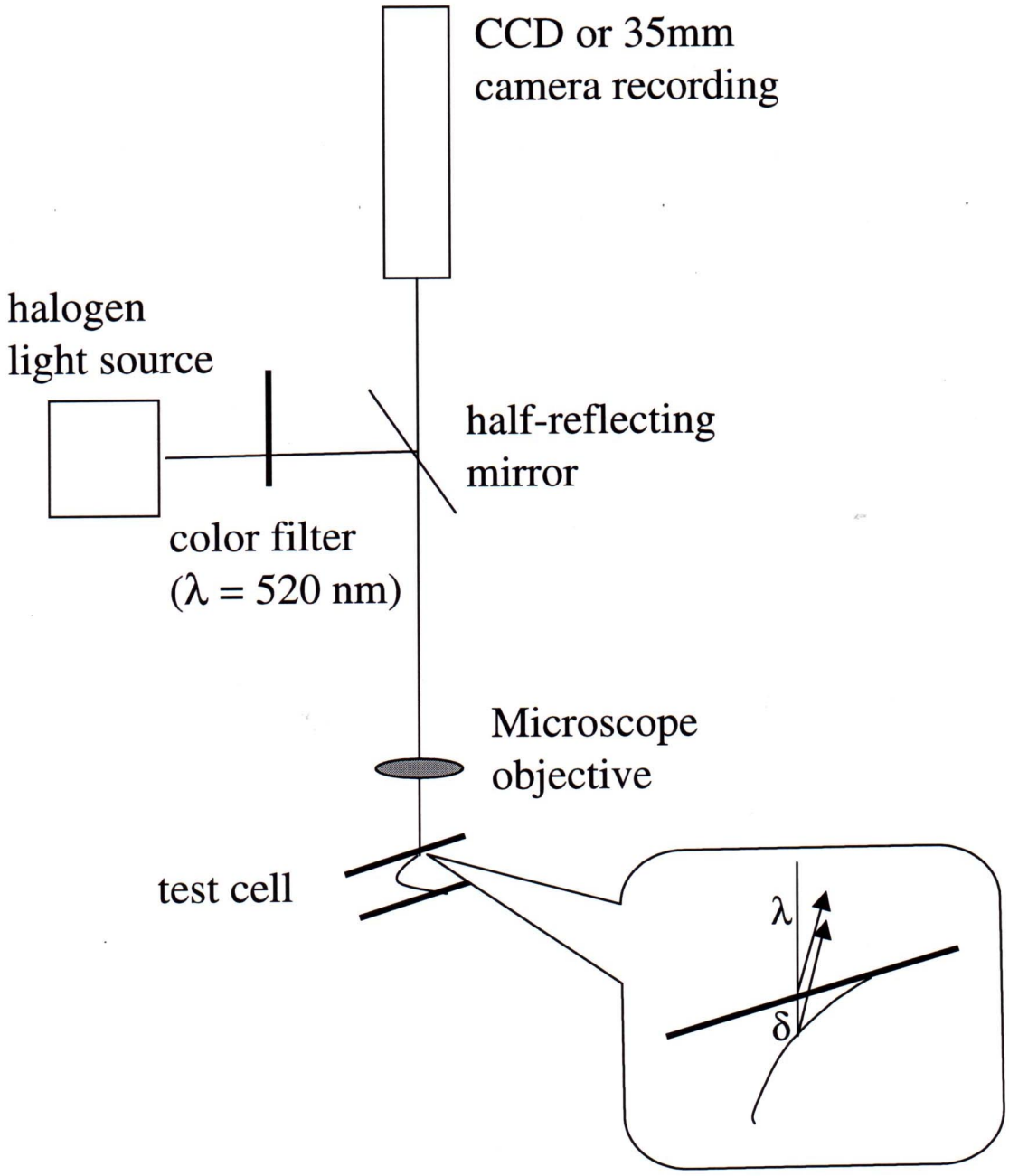

Fig. 3 Fizeau interferometry

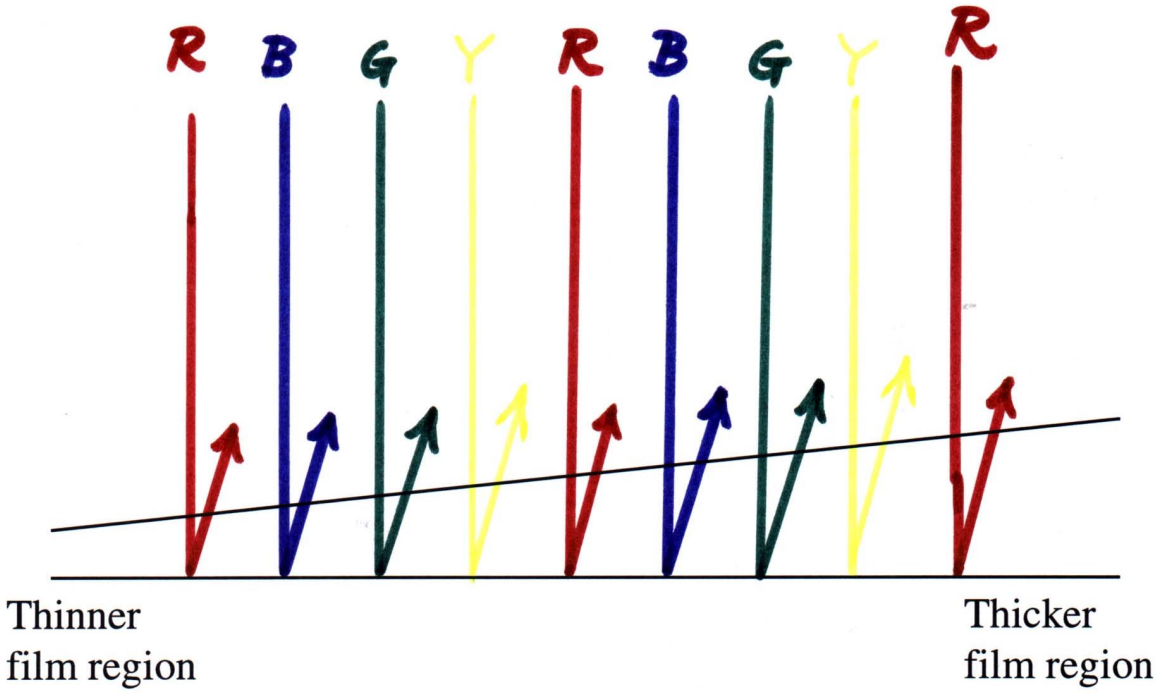

Fig. 4 Schematic illustration of color-shifted Fizeau fringes

(a)

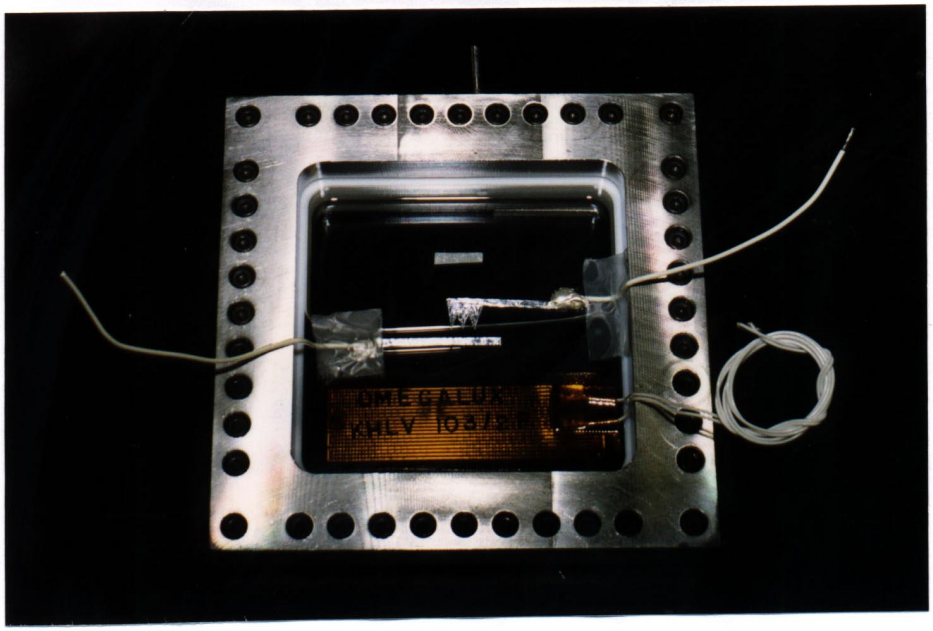

(b)

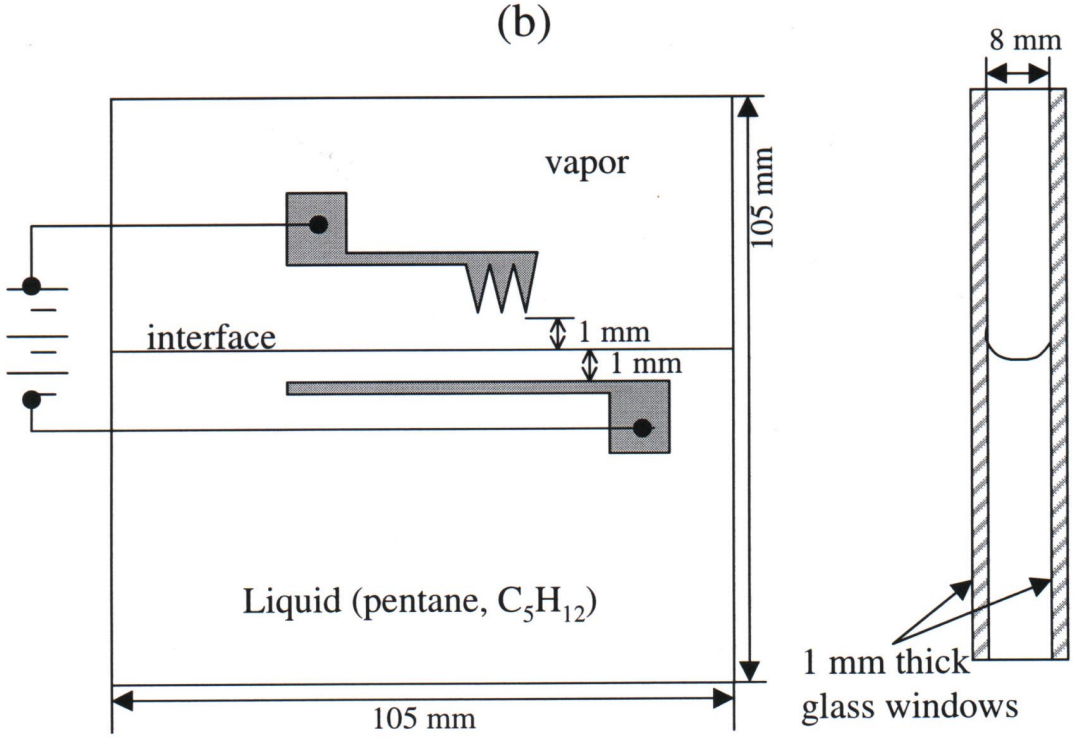

Fig. 5 Test cell configuration

Fig. 6 Fizeau Fringes of Thin Meniscus

(a) $\lambda = 520$ nm

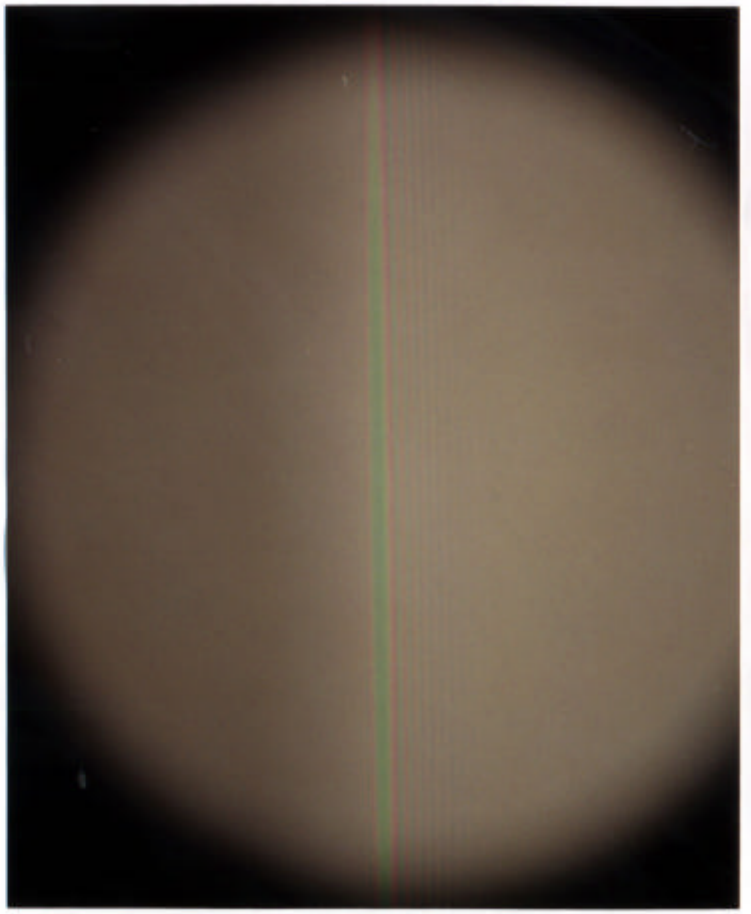

(b) White light

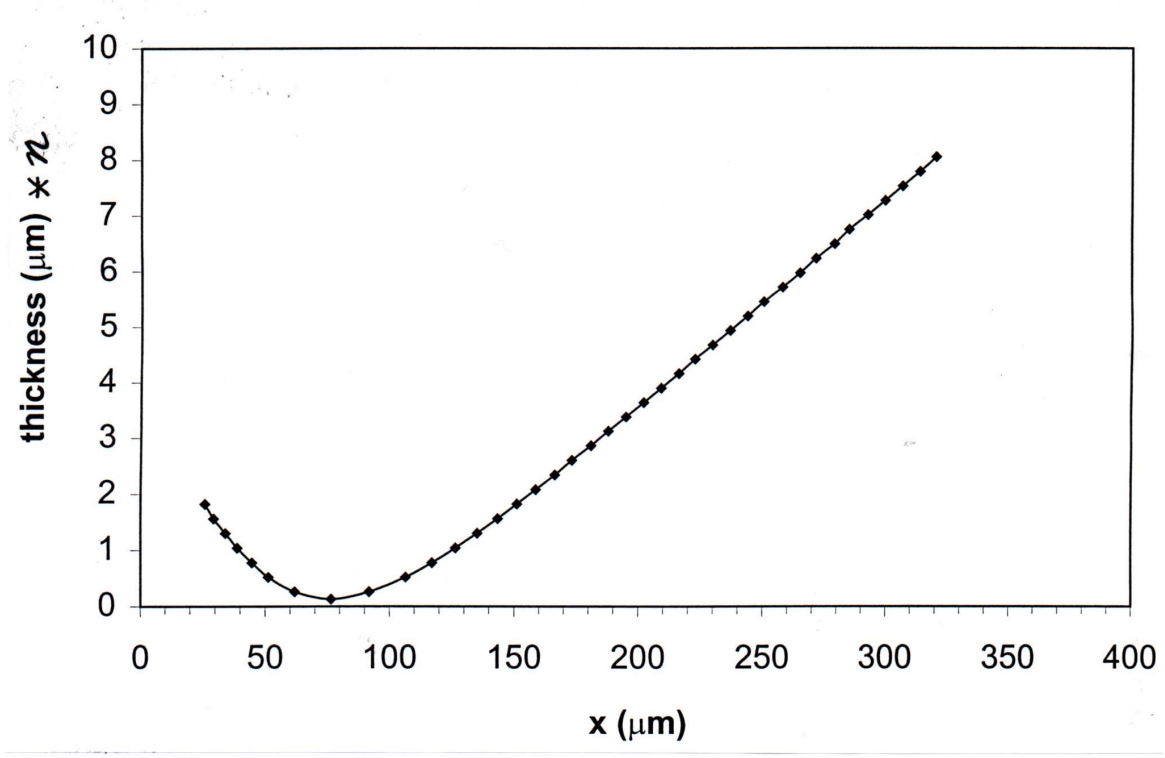

Fig. 7 Thickness contour of nonevaporating thin film region (index of refraction of pentane $n_{pentane} = 1.357$).

(a) $Q = 0, V_{ch} = 0$

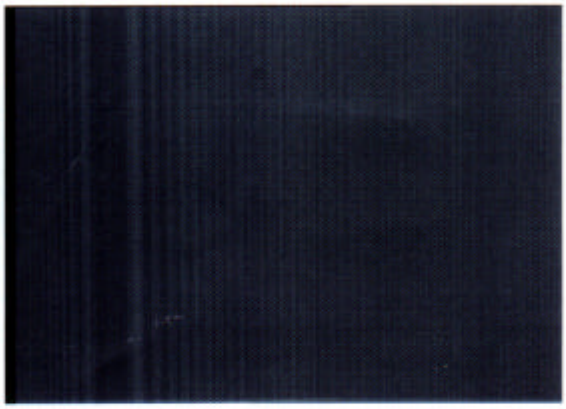

(b) $Q = 0.2$ watts, $V_{ch} = 0$

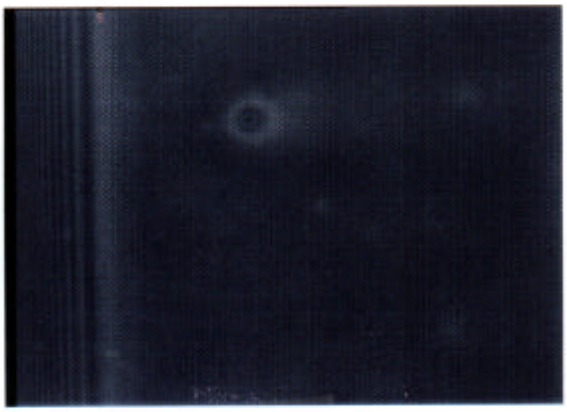

(c) $Q = 0.2$ watts; $V_{ch} = 1.5$ kV

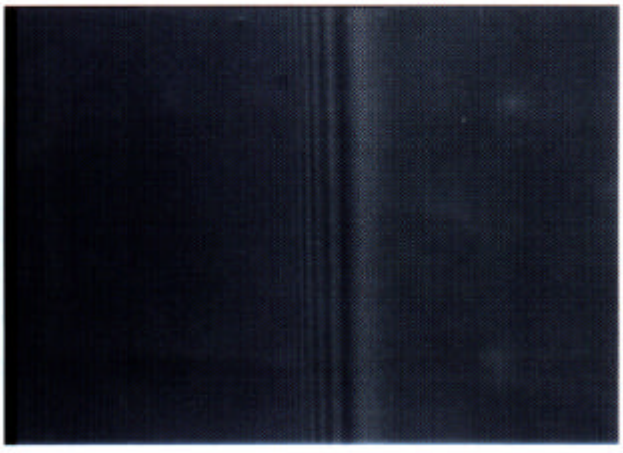

Fig. 8 Fizeau fringes for thin liquid films under different heating and electric charging conditions.

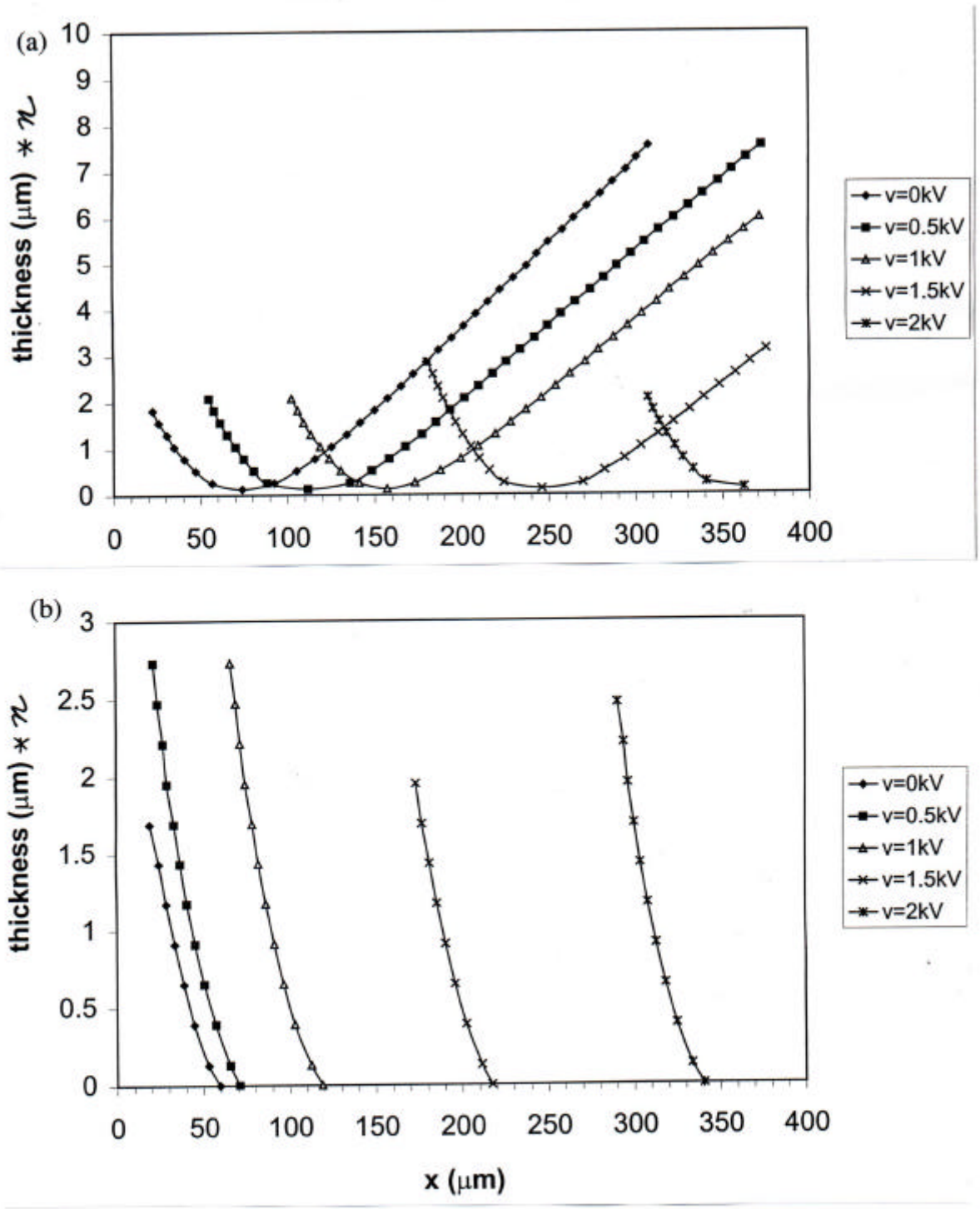

Fig. 9 Electrophoresis movement of thickness contours of (a) nonevaporating; and (b) evaporating thin film regions.